

Linear stability of electrodynamic tethers

M. DOBROWOLNY

CNR, Istituto di Fisica Spazio Interplanetario - Rome, Italy

(ricevuto il 25 Gennaio 2001; revisionato il 22 Febbraio 2002; approvato il 25 Marzo 2002)

Summary. — We investigate the dynamic stability of electrodynamic tethers of the type envisaged for future applications like deorbiting spacecraft and/or propulsion. In such tethers, electrodynamic forces couple the tether natural oscillations in the orbital plane with those out of the orbital plane. The investigation is done with reference to a model where the time variation of the tether current is assumed to be given. In addition, we address both the case of a bare tether and that of an insulated conducting tether collecting current through a terminating balloon. In the linear approximation, we find possible instabilities of the tether libration modes, at moderate current values, for both the case of a bare tether and that of an insulated conducting tether. Instabilities are also found for the lateral oscillations (string modes) and the case of a bare tether. The equations obtained allow a discussion of the instability mechanisms.

PACS 94.20.-y – Physics of the ionosphere.

1. – Introduction

Electrodynamic tethered systems are functioning on the basis of the electrodynamic potential (e.m.f.) which arises as a consequence of the motion of the conducting tether through the Earth's magnetic field. A tether deployed upwards, and moving eastwards, charges positively with respect to the ionosphere towards the top and, in a passive case, negatively towards the bottom. This causes current circulation in the tether.

Future applications of electrodynamic tethers go essentially in two directions (both using the current circulating in the conducting tether). The first, which is significant especially in connection with the International Space Station, is that of using this current to obtain propulsion. For that purpose, one needs to reverse the natural direction of current in the tether through the use of a power supply which overcomes the motional e.m.f.

The second application, which is important with respect to the problem of accumulation of debris in Near Earth's orbits [1], is that of using electrodynamic tethers to deorbit LEO objects (either satellites or rocket upper stages). In this case, one uses the fact that, associated with the natural current in the tether, there is an electrodynamic drag force

which, indeed, lower its orbit. Several investigations on such electrodynamic deorbiting have been performed recently [2, 3], for different system configurations (both bare and insulated tethers with and without a conducting balloon at the upper end), with very promising results concerning the deorbiting times.

A NASA test mission on electrodynamic deorbiting, called ProSEDS [4], is under preparation and will fly in the year 2001. There an electrodynamic tether system will be used to deorbit the upper stage of a Delta rocket from an initial (circular) orbit at 400 km of altitude.

For both the applications mentioned above (*i.e.* propulsion and electrodynamic deorbiting), one obviously needs to have significant currents in the tether to enhance the electrodynamic forces. Because of this, the electrodynamic forces may become significant with respect to gravity gradient forces and a crucial problem to investigate is that of the stability of the system.

Notice that, already in the years of preparation of the TSS missions [5], several investigations were performed with the goal of devising means of controlling tether oscillations (see, for example, ref. [6]). However, these analyses were not taking into account the electrodynamic forces. More recent simulations [7], including electrodynamic forces and referred to the ProSEDS mission, do show the onset of instability of tether transverse oscillations during the orbital motion of the system.

If there are instabilities, as these simulations indicate, it is imperative to try to understand the corresponding physical mechanisms in such a way as to be able to exercise some control law. On the other hand, it would be certainly difficult to obtain such an understanding out of complex numerical simulations (like those of ref. [7]), involving realistic ionospheric and atmospheric models as well as thermal models of the tether, and referring to a specific mission (and, therefore, to a specific tether system).

For this reason, we will approach in this paper the problem of tether stability in a different way by imposing, rather than calculating self-consistently, a reasonable model for the time variation of the electrical current in the tether and then studying the equations for in-plane and out-of-plane oscillations of the tether in a mostly analytical way.

A similar approach has indeed been followed in two recent papers [8, 9] in which, however, the current in the tether was assumed to be constant in time (and along the tether length). Furthermore, ref. [8] deals with the case of a rigid tether, while ref. [9] simulates tether flexibility by using a two-bar model for the tether. In both cases the dynamics is described by ordinary differential equations in time.

The analysis that we present in this paper is more realistic. First of all, we refer from the beginning to a truly flexible tether, analyzing therefore a system of partial differential equations (the independent variables being time and the coordinate along the vertical). Secondly, we allow for a variation of current with time simulating the tether response to the time variations of the ionospheric electron density. Finally, we do the analysis for two different tether configurations. The first is an insulated conducting tether collecting current through a conducting balloon at one of its terminations and the second is a bare tether collecting current from the ionosphere all along its length. In the second case, the current, besides varying in time, is allowed to vary, as in fact does, along the tether length.

The analysis is however limited to the linear approximation in the amplitude of tether oscillations, so that the effect of non-linearities (which might be important on account of the results in ref. [8]) cannot be predicted.

The paper is organized as follows. In sect. 2 we write and discuss the basic equations of the lateral oscillations of a flexible tether in the presence of electrodynamic forces. It

is seen that electrodynamic forces couple in-plane and out-of-plane oscillations (which are uncoupled in the absence of current) and it is this coupling which eventually induces instability of various modes.

In sect. **3** we present the models that we are using for the tether current, appropriate to the two configurations mentioned above, and the corresponding dynamical equations. In sect. **4** we address the problem of librations and derive, out of the original system of partial differential equations, a problem differential in time only (for both the bare and the insulated tether). In sect. **5** we address the problem of higher-frequency lateral oscillations (*i.e.* the string modes) and, as in the case of librations, derive a system of ordinary differential equations in time. Section **6** is a discussion of the mechanisms driving instabilities, for both librations and lateral modes. Sections **7** and **8** contain numerical results for the libration and for the lateral modes, respectively. Finally, sect. **9** summarizes and discusses the results that we have found.

2. – Basic equations for tether oscillations

The system we refer to is made up of a satellite (mass m_s) with attached a conducting tether (mass m_t) deployed upwards and terminated with a ballast mass m_b . Supposing $m_s \gg (m_b, m_t)$, the center-of-mass of the tether system will be located at the spacecraft. We refer, in all the treatment, to a circular orbit and choose a coordinate system with origin in the center of mass of the tether system, the x -axis pointing in the direction of orbital motion, the z -axis along the vertical (directed away from the Earth's center) and the y -axis out of the orbital plane and directed in such a way as to obtain a right-handed coordinate system.

We identify the position of a tether element ds , at a given time t , by coordinates $(\xi, \eta, \zeta = z + u)$, where $(0, 0, z)$ would be the position of that element with the tether along the vertical (the equilibrium position in the presence of gravity gradient forces only).

The tether transverse oscillations (*i.e.* oscillations in a plane perpendicular to z) will be characterized by certain functions $\xi(z, t)$, $\eta(z, t)$. Alternatively, we can describe such oscillations in terms of two angles $\alpha_{\text{in}}(z, t)$ and $\alpha_{\text{out}}(z, t)$. Of these, α_{in} is the angle with respect to the vertical of the projection on the orbital plane of the local tangent to the tether element ds and α_{out} is the inclination of the same local tangent with respect to the orbital plane.

In a linear approximation in the amplitudes of the angles α_{in} and α_{out} , which will be used all along this paper, we have

$$(1) \quad \frac{dz}{ds} \sim 1, \quad \alpha_{\text{in}} \sim \xi_z, \quad \alpha_{\text{out}} \sim \eta_z,$$

while it is seen that the longitudinal oscillations u are second order in the angles. Here, and in the following, the suffix z denotes partial derivative with respect to z , *i.e.* for example $\xi_z = \partial\xi/\partial z$, etc.

In such a linear approximation, the equations for the in-plane and out-of-plane displacements ξ and η are uncoupled from the equation for the longitudinal displacements u and can be written as

$$(2) \quad \ddot{\xi} = p\tilde{\xi}_{zz} + \alpha f_{ex}, \quad \ddot{\eta} + \tilde{\eta} = p\tilde{\eta}_{zz} + \alpha f_{ey}.$$

Here the dot represents derivative with respect to a normalized time

$$\tau = \omega_0 t,$$

ω_0 being the orbital frequency ($\omega_0 = 1.16 \times 10^{-3}$ rad/s for a circular orbit at 400 km of altitude) and all lengths are normalized to the tether length L (*i.e.* $\tilde{\xi} = \xi/L$, etc.). It is, furthermore,

$$(3) \quad p = \frac{3 + \mu}{\mu}, \quad \mu = \frac{m_t}{m_b}.$$

The terms proportional to α are the x and y components of the electrodynamic force. Equations (2), with $\alpha = 0$, can be found in several places in the literature on tether dynamics [10,11]. In particular, in ref. [11], a derivation is given which takes into account also high-frequency longitudinal oscillations of the tether.

From the analysis of ref. [2], which refers to the case of a dipole model for the Earth's magnetic field, we obtain, for the electrodynamic terms,

$$(4) \quad \alpha = \frac{B_0 I}{m_t \omega_0^2}$$

with B_0 the Earth's magnetic field (depending on altitude), and

$$(5) \quad f_{ex} = -[\cos \lambda + 2\eta_z \sin \lambda \sin \theta], \quad f_{ey} = \sin \lambda [\cos \theta + 2\xi_z \sin \theta].$$

Here λ is the inclination of the orbit with respect to the magnetic equator and θ the orbital anomaly measured from the intersection of the plane of the orbit with the plane of the magnetic equator ($\theta = \omega_0 t = \tau$).

The current I depends on time because it follows the variations in the ionospheric density and (in the case of a bare tether), also because it depends on the local angles α_{in} , α_{out} which, in turn, depend on time. Further time dependences (in α) would be obtained with a more refined model of the Earth's magnetic field including harmonics higher than the dipole. However, the amplitudes of even the first-harmonic components are smaller (by a factor ~ 10) than the amplitude of the dipole [12], so that we believe that their effect will be smaller than that obtained from the day-night variation of the ionospheric density.

From eqs. (5), we see that the electrodynamic forces act on the dynamics of transverse oscillations in two different ways. First of all, they provide source terms (not depending on ξ , η) in the equations. Secondly, they couple the in-plane and the out-of-plane oscillations (for $\lambda \neq 0$). It is important to notice that this coupling involves the first derivatives (with respect to \tilde{z}) of the displacements, *i.e.* ξ is coupled to η_z and η is coupled to ξ_z . This implies that the parity, with respect to \tilde{z} , of the dynamical terms in eqs. (2), is opposite with respect to the parity of the terms giving the electrodynamic coupling.

Let us now discuss the boundary conditions at the two tether terminations $\tilde{z} = 0$ and $\tilde{z} = 1$ to be associated with eqs. (2). In both cases we have to impose that the tether tension equals the total force on the corresponding mass plus its acceleration. The tether tension can be written [11] as

$$\underline{F}_t = L m_t \omega_0^2 \hat{i}_s,$$

with

$$\hat{i}_s = [\xi_z \hat{i}_x + \eta_z \hat{i}_y + (1 + u_z) \hat{i}_z] \frac{dz}{ds}$$

the unit vector along the tether direction and

$$\omega_t^2 = p\omega_0^2.$$

As we will see, ω_t is a frequency characterizing the tether lateral oscillations, while the tether librations have frequencies of order ω_0 . At the ballast mass ($\tilde{z} = 1$), the balance between tension force and total force plus acceleration can therefore be written (for the x and y directions) as

$$Lm_t \omega_t^2 [\xi_z \hat{i}_x + \eta_z \hat{i}_y]_1 = [-m_b L \omega_0^2 \ddot{\xi} + F_{ex}]_1 \hat{i}_x + [-m_b L \omega_0^2 (\ddot{\eta} + \tilde{\eta}) + F_{ey}]_1 \hat{i}_y,$$

where the index 1 denotes that all quantities have to be evaluated at $\tilde{z} = 1$ and $F_{ex}(1)$ and $F_{ey}(1)$ are the x and y components of a possible electrodynamic force at the ballast mass. For this electrodynamic force, we can write

$$\underline{F}_e(1) = IB_0(\hat{i}_s \times \underline{b}) \Delta l_b,$$

where we have assumed the ballast mass to be equivalent to a tether element of length Δl_b and the vector \underline{b} is given by [2]

$$\underline{b} \equiv (3 \sin \lambda \sin \theta \cos \theta, \quad 3 \sin \lambda \sin^2 \theta \cos \lambda, \quad 3 \sin^2 \theta \sin^2 \lambda - 1).$$

For a bare tether, it is $I = 0$ at the ballast mass termination. For an insulated tether with a conducting balloon at $z = 1$, we will have $\Delta l_b \sim r_b$ with r_b the radius of the balloon. As $r_b \ll L$, excluding the case of enormous currents, F_{ex} and F_{ey} will be negligible in comparison with the remaining terms in the balance conditions. Thus, for both configurations, we derive for the boundary conditions at $\tilde{z} = 1$

$$\ddot{\xi}(1) + \mu p \xi_z(1) = 0, \quad \ddot{\eta}(1) + \tilde{\eta}(1) + \mu p \eta_z(1) = 0,$$

or, making use of eq. (2) written in $\tilde{z} = 1$,

$$(6) \quad [\tilde{\xi}_{zz} + \mu \tilde{\xi}_z]_1 = 0, \quad [\tilde{\eta}_{zz} + \mu \tilde{\eta}_z]_1 = 0.$$

On the other hand, at the satellite end ($\tilde{z} = 0$), because of the high satellite mass, it is reasonable to suppose that the termination of the tether anchored to the satellite does not move (except for following the satellite motion). The boundary conditions at $\tilde{z} = 0$ will therefore be

$$(7) \quad \tilde{\xi}(0) = \tilde{\eta}(0) = 0.$$

Before proceeding to an analysis of the effects of the electrodynamic forces, it is useful to recall what we obtain from eqs. (2) when $\alpha = 0$ (*i.e.* $I = 0$). Seeking the solutions in the form

$$(8) \quad \tilde{\xi}(\tilde{z}, t) = \sin(k\tilde{z})x(t), \quad \tilde{\eta}(\tilde{z}, t) = \sin(k\tilde{z})y(t)$$

which satisfy the boundary conditions (7), we obtain a differential problem (in t only) for $x(t)$ and $y(t)$ given by

$$(9) \quad \ddot{x} + k^2 p x = 0, \quad \ddot{y} + (1 + k^2 p) y = 0,$$

where k will have to be determined through the boundary conditions (6) at $\tilde{z} = 1$. Introducing there the ansatz (8) leads to the following dispersion equation for k (excluding the solution $k = 0$):

$$-k \sin(k) + \mu \cos(k) = 0.$$

This has a solution

$$(10) \quad k_0^2 \sim \mu$$

corresponding to $k \ll 1$, and also an infinite number of other solutions with

$$(11) \quad k \equiv k_n \sim n\pi + \frac{\mu}{n\pi}, \quad n = 1, 2, \dots$$

Using (10), eqs. (9) become

$$\ddot{x} + (3 + \mu)x = 0, \quad \ddot{y} + (4 + \mu)y = 0,$$

so that we recognize (if we neglect μ), the typical frequencies $\sqrt{3}\omega_0$ and $2\omega_0$ of the rigid pendulum. There is a correction to these frequencies (due to μ) and, in addition, the wire is not rigid but bended according to the law $\sin(\sqrt{\mu}\tilde{z})$.

On the other hand, the solutions (11) for k represent the true lateral oscillations of the string with both ends fixed at frequencies (normalized to ω_0) which are multiples of $\pi\sqrt{p}$ (with, again, a correction proportional to μ). From the definition (3) of p , we see that, for $m_t \ll m_b$ (as will be usually the case), it is $p \gg 1$ and, hence, the lateral frequencies (starting from the fundamental mode $n = 1$) will be higher than the libration frequencies.

If we now turn to the complete problem (2) including electrodynamic forces, we see however that an ansatz like (8) for ξ and η does not work because ξ_z and η_z on the right-hand sides of the equations would give terms proportional to $\cos k\tilde{z}$ which cannot be matched with the remaining terms in the equations. This has obviously to do with the fact, already remarked, that the parity of the terms giving electrodynamic coupling is opposite to that of the dynamical terms.

3. – Models for the tether current and corresponding dynamical equations

In general, the current has to be computed self-consistently, while the tether is orbiting (and oscillating) through the Earth's ionosphere. For the purpose of this paper, which is addressed to fundamentals of tether dynamics in the presence of electrodynamic forces, the time dependence of the current will however be given. More precisely, we will use two models which are appropriate for the two cases of an insulated conducting tether which is collecting current through a conducting balloon at one of its terminations and the case of a bare metallic tether.

3.1. Insulated conducting tether. – For an insulated conducting tether, the current is constant along the tether length and depends only on time, its time variation being induced by the ionospheric density variation. The real ionosphere will of course exhibit a spectrum of frequencies with different amplitudes. Among them, however, a basic frequency will be that associated to the day-night variation which will be equal to the orbital frequency ω_0 . Consequently, we will take, as our model for the current relevant to the case of an insulated tether

$$(12) \quad I = I_0 [1 + \delta \sin (\omega_0 t + \phi)].$$

The phase ϕ in eq. (12) is a phase with respect to the orbital motion $\theta = \omega_0 t$. As the current in the tether, once it is switched on, follows obviously the day-night ionospheric variation, the phase ϕ will be determined only by the orbit of the system under consideration (and will vary while the orbit rotates around the Sun).

Notice also that, in the electrodynamic terms of eqs. (2), also the orbital inclination λ varies with time and can be expressed as

$$(13) \quad \lambda = j + \phi_b \sin (\omega_m t),$$

where j is the inclination of the orbit over the Earth’s equator and $\phi_b = 11.5^\circ$. This variation is on a period $T = 2\pi/\omega_m = 1$ day, which is much longer than the orbital period, and, in most cases, will be neglected in the following treatment.

Corresponding to (12), we will write in eqs. (2)

$$\alpha = \epsilon s(t)$$

with

$$(14) \quad \epsilon = \frac{B_0 I_0}{m_t \omega_0^2}, \quad s(t) = 1 + \delta \sin (\omega_0 t + \phi).$$

With that, only two dimensionless parameters (ϵ and μ) appear in eqs. (2) governing the tether dynamics.

Like in the case $I = 0$, the tether modes of oscillation will be a superposition of libration modes (low frequency) and of lateral modes at higher frequencies. We will therefore write in general

$$(15) \quad \xi(\tilde{z}, t) = \xi_0(\tilde{z}, t) + \xi_1(\tilde{z}, t), \quad \eta(\tilde{z}, t) = \eta_0(\tilde{z}, t) + \eta_1(\tilde{z}, t),$$

where we simply refer with an index “0” to the libration modes and with an index “1” to the lateral modes. These lateral modes will in turn be an infinity of modes at frequencies which are integer multiples of $\pi\sqrt{p}$.

If we substitute (15) in eqs. (2) and then average over times of the order of the period of the high-frequency oscillations, we remain with

$$(16) \quad \begin{aligned} \ddot{\xi}_0 &= p\tilde{\xi}_{0zz} - \epsilon s(t) [\cos \lambda + 2\eta_{0z} \sin \lambda \sin \theta], \\ \ddot{\eta}_0 + \tilde{\eta}_0 &= p\tilde{\eta}_{0zz} + \epsilon s(t) [\sin \lambda \cos \theta + 2\xi_{0z} \sin \lambda \sin \theta]. \end{aligned}$$

Notice that the source terms in eqs. (2) survive the average, while the parts proportional to η_{1z} and ξ_{1z} of the coupling terms average out to zero. The resulting equations (16) contain therefore libration modes only.

On the other hand, subtracting (16) from (2), we remain with the problem of lateral modes given by

$$(17) \quad \begin{aligned} \ddot{\xi}_1 &= p\tilde{\xi}_{1zz} - 2\epsilon s(t)\eta_{1z} \sin \lambda \sin \theta, \\ \ddot{\eta}_1 + \tilde{\eta}_1 &= p\tilde{\eta}_{1zz} + 2\epsilon s(t)\xi_{1z} \sin \lambda \sin \theta. \end{aligned}$$

Thus the lateral mode problem, in our linear approximation, will be a homogeneous problem.

3.2. Bare tether. – For the case of a bare tether, the current does vary along the tether length. Using the theory of OML current collection [13], we obtain for the tether current

$$I(\tilde{z}, t) = i_0(t) \int_{\tilde{z}}^1 dz' [1 + \tilde{\Phi}(z')]^{1/2}$$

with

$$i_0(t) = \frac{\pi}{2} n(t) e v_{\text{the}} L r_w, \quad \tilde{\Phi} = e\Phi/kT_e$$

r_w being the tether radius, v_{the} the electron thermal velocity and $n(t)$ the electron density. Disregarding the tether electrical resistance, it is [2]

$$\tilde{\Phi}(\tilde{z}, \tau) = \tilde{\Phi}_0 \int_0^{\tilde{z}} dz' \left[\cos \lambda \cos \alpha_{\text{in}} \cos \alpha_{\text{out}} + 2 \sin \lambda \sin \tau \sin \alpha_{\text{out}} \right]$$

with $\Phi_0 = V_0 B_0 L$ and V_0 the orbital velocity. With that, in the linear approximation, and for $\tilde{\Phi} \gg 1$, we obtain for the current

$$(18) \quad I(\tilde{z}, \tau) = \frac{2}{3} (\cos \lambda)^{1/2} I_0 \frac{n(t)}{n_0} \left[(1 - z^{3/2}) + \frac{3}{2} I_1^t \tan \lambda \sin \tau \right],$$

where $n(t)$ is the electron density, n_0 is its average value, and

$$(19) \quad I_0 = \frac{\pi}{2} e n_0 v_{\text{the}} r_w L \tilde{\Phi}_0^{1/2}.$$

Furthermore, we have introduced

$$I_1^t = \int_{\tilde{z}}^1 dz' \frac{\eta}{(z')^{1/2}}.$$

Assuming now, in analogy with (12), a sinusoidal variation for the ionospheric density, *i.e.* writing

$$n(t) = n_0 [1 + \delta \sin(\omega_0 t + \phi)]$$

and using eq. (18) for the current in eqs. (2), we end up, in the linear approximation, with

$$(20) \quad \begin{aligned} \ddot{\xi} &= p\tilde{\xi}_{zz} - \epsilon_0 s(t) \left[(1 - \tilde{z}^{3/2}) (\cot \lambda + 2\eta_z \sin \theta) + \frac{3}{2} I_1^l \sin \theta \right], \\ \ddot{\eta} + \tilde{\eta} &= p\tilde{\eta}_{zz} + \epsilon_0 s(t) \left[(1 - \tilde{z}^{3/2}) (\cos \theta + 2\xi_z \sin \theta) + \frac{3}{4} I_1^l \tan \lambda \sin (2\theta) \right], \end{aligned}$$

where

$$(21) \quad \epsilon_0 = \frac{2}{3} \epsilon (\cos \lambda)^{1/2} \sin \lambda.$$

Introducing now the superposition (15) of librations and lateral modes in eqs. (20), and then averaging the resulting equations over the shorter time scales of the lateral modes, we obtain for librations

$$(22) \quad \begin{aligned} \ddot{\xi}_0 &= p\tilde{\xi}_{0zz} - \epsilon_0 s(t) \left[(1 - \tilde{z}^{3/2}) (\cot \lambda + 2\eta_{0z} \sin \theta) + \frac{3}{2} I_{10}^l \sin \theta \right], \\ \ddot{\eta}_0 + \tilde{\eta}_0 &= p\tilde{\eta}_{0zz} + \epsilon_0 s(t) \left[(1 - \tilde{z}^{3/2}) (\cos \theta + 2\xi_{0z} \sin \theta) + \frac{3}{4} I_{10}^l \tan \lambda \sin (2\theta) \right], \end{aligned}$$

where

$$I_{10}^l = \int_{\tilde{z}}^1 dz' \frac{\eta_0}{(z')^{1/2}}.$$

As for the higher-frequency lateral modes, we obtain the equations

$$(23) \quad \begin{aligned} \ddot{\xi}_1 &= p\xi_{1zz} - 2\epsilon_0 s(t) \sin \theta \left[(1 - \tilde{z}^{3/2}) \eta_{1z} + \frac{3}{4} I_{11}^l \right], \\ \ddot{\eta}_1 + \eta_1 &= p\eta_{1zz} + 2\epsilon_0 s(t) \sin \theta \left[(1 - \tilde{z}^{3/2}) \xi_{1z} + \frac{3}{4} I_{11}^l \tan \lambda \cos \theta \right] \end{aligned}$$

with

$$I_{11}^l = \int_{\tilde{z}}^1 dz' \frac{\eta_1}{(z')^{1/2}}.$$

Notice that there is no coupling between librations and lateral modes in our treatment (due to their frequency separation). Both problems are linear and the only coupling we will be talking about, in both problems, will be that between in-plane and out-of-plane modes.

4. – Librations

In this section we will address the libration modes in the presence of electrodynamic forces for the two models of the tether current illustrated in sect. 3. Starting from the original problem (see eqs. (16) or (22)), which is a partial differential problem, we will manage to obtain a system of ordinary differential equations in time only.

4.1. *Insulated tether.* – For $I = 0$, the case of librations was derived from the ansatz (8) seeking solutions for $k \ll 1$. Notice that, for $k \ll 1$, the ansatz (8) corresponds to a polynomial in \tilde{z} containing only odd powers of \tilde{z} and that cannot be used for $I \neq 0$, because the odd powers of \tilde{z} on the left-hand sides of eqs. (16) would give even powers of \tilde{z} in the electrodynamic coupling terms. We will therefore modify the ansatz (8) to

$$(24) \quad \tilde{\xi}_0(\tilde{z}, t) = \sum_{n=1}^{\infty} \tilde{z}^n x_n(t), \quad \tilde{\eta}_0(\tilde{z}, t) = \sum_{n=1}^{\infty} \tilde{z}^n y_n(t),$$

i.e. to that of an infinite series containing all powers of \tilde{z} . Inserting that into eqs. (16) and then equating equal powers of \tilde{z} in both equations, we obtain, from the terms which are constant with respect to \tilde{z} ,

$$(25) \quad \begin{aligned} 0 &= 2px_2 - \epsilon s(t) [\cos \lambda + 2y_1 \sin \lambda \sin \theta], \\ 0 &= 2py_2 + \epsilon s(t) [\sin \lambda \cos \theta + 2x_1 \sin \lambda \sin \theta], \end{aligned}$$

while, for $n \geq 1$,

$$(26) \quad \begin{aligned} \ddot{x}_n &= p(n+2)(n+1)x_{n+2} - 2\epsilon s(t) \sin \lambda \sin \theta y_{n+1}, \\ \ddot{y}_n + y_n &= p(n+2)(n+1)y_{n+2} + 2\epsilon s(t) \sin \lambda \sin \theta x_{n+1}. \end{aligned}$$

Notice that eqs. (25) are equivalent to impose that the original equations (16) are verified in $\tilde{z} = 0$.

To the above set of (ordinary) differential equations for the x'_n 's and y'_n 's, we have to add the boundary conditions (6) in $\tilde{z} = 1$ which, using (24), can be rewritten as

$$(27) \quad \mu x_1 + \sum_{m=2}^{\infty} a_m x_m = 0, \quad \mu y_1 + \sum_{m=2}^{\infty} a_m y_m = 0$$

with

$$a_m = m(m-1 + \mu).$$

The method we have sought to investigate the solution to this problem is the following. Suppose we stop the infinite polynomials (24) to the power n_0 . Then the boundary conditions (27), truncated at $m = n_0$, can be solved with respect to x_{n_0}, y_{n_0} . Going then to eqs. (26), written for $n = n_0 - 2$, we can solve them with respect to x_{n_0-1}, y_{n_0-1} . These can be used in eqs. (26) again, written now for $n = n_0 - 3$, and so on, until we arrive at the equations corresponding to $n = 1$, which are

$$(28) \quad \begin{aligned} \ddot{x}_1 &= 6px_3 - 4\epsilon s(t)y_2 \sin \lambda \sin \theta, \\ \ddot{y}_1 + y_1 &= 6py_3 + 4\epsilon s(t)x_2 \sin \lambda \sin \theta. \end{aligned}$$

In these equations, through the previous procedure, we will have obtained x_3 and y_3 expressed in terms of x_1, y_1, x_2, y_2 , so that, combining with eqs. (25), we will have a closed problem.

Obviously, by varying n_0 , *i.e.* by varying the power at which we stop the polynomial ansatz (24), we will end up with different expressions for x_3, y_3 (in terms of $x_1, y_1, x_2,$

y_2) to use in eqs. (28) and the method will work only if, upon increasing n_0 , the results for x_3, y_3 will differ less and less.

This is in fact what we find to occur. Without reporting calculations (see ref. [14]), we find that, going beyond a cubic ansatz for $\xi_0, \tilde{\eta}_0$, introduces corrections which are negligible except for unreasonably high currents (> 10 A for the typical tethers we can consider for deorbiting). On the other hand, with a cubic ansatz for $\xi_0, \tilde{\eta}_0$, and using the procedure outlined, we end up with the following system of equations coupling x_1 and y_1 :

$$(29) \quad \ddot{x}_1 + \left(\omega_l^2 - \frac{4}{p} \epsilon^2 s(t)^2 \sin^2 \lambda \sin^2 \theta \right) x_1 = -\frac{6a_2}{a_3} \epsilon s(t) y_1 \sin \lambda \sin \theta + S(t),$$

$$\ddot{y}_1 + \left(1 + \omega_l^2 - \frac{4}{p} \epsilon^2 s(t)^2 \sin^2 \lambda \sin^2 \theta \right) y_1 = \frac{6a_2}{a_3} \epsilon s(t) x_1 \sin \lambda \sin \theta + R(t).$$

Here we have denoted with $S(t)$ and $R(t)$ the source terms (not containing x_1 and y_1) in the two equations given by

$$S(t) = -\frac{3a_2}{a_3} \epsilon s(t) \cos \lambda + \frac{1}{p} \epsilon^2 s(t)^2 \sin^2 \lambda \sin(2\theta),$$

$$R(t) = \frac{3a_2}{a_3} \epsilon s(t) \sin \lambda \cos \theta + \frac{1}{p} \epsilon^2 s(t)^2 \sin(2\lambda) \sin \theta.$$

Furthermore, the frequency ω_l (normalized to ω_0) is defined by

$$(30) \quad \omega_l^2 = \frac{6p\mu}{a_3} = \frac{2(3 + \mu)}{2 + \mu},$$

so that, for $\mu \ll 1$, we obtain $\omega_l \sim \sqrt{3}$ which is the frequency of the in-plane oscillations of the rigid pendulum.

4.2. *Bare tether.* – The relevant equations are now eqs. (22). Using the expansion (24) for ξ_0, η_0 , and then equating equal powers of \tilde{z} is, however, not possible here because the electrodynamic terms contain half integral powers of \tilde{z} . To proceed analytically, and with the same method used in subsect. 4.1, we approximate the term $1 - \tilde{z}^{3/2}$ with $1 - \tilde{z}$ and substitute $t^{1/2}$ with t in the integral I_{10}^l . With that, we can again equate equal powers of \tilde{z} in eqs. (22). Limiting ourselves to the cubic approximation for ξ_0 and η_0 , we end up with the following equations for x_1, y_1 :

$$(31) \quad \ddot{x}_1 + \Omega_1^2 x_1 = S(t) + \frac{7}{2} \epsilon_0 s(t) y_1 \sin \theta \left[1 - \frac{3a_2}{a_3} + \frac{3}{7p} \epsilon_0 s(t) \tan \lambda \sin(2\theta) \right],$$

$$\ddot{y}_1 + \Omega_2^2 y_1 = R(t) - 2\epsilon_0 s(t) \left(1 - \frac{3a_2}{a_3} \right) x_1 \sin \theta,$$

where we have introduced

$$\Omega_1^2 = \omega_l^2 - \frac{4}{p} \epsilon_0^2 s(t)^2 \sin^2 \theta,$$

$$\begin{aligned}\Omega_2^2 &= 1 + \omega_l^2 + \frac{3}{4}\epsilon_0 s(t) \left(1 - \frac{3a_2}{a_3}\right) \tan \lambda \sin(2\theta) - \frac{7}{2p}\epsilon_0^2 s(t)^2 \sin^2 \theta, \\ S(t) &= \epsilon_0 s(t) \cot \lambda \left(1 - \frac{3a_2}{a_3}\right) + \frac{1}{p}\epsilon_0^2 s(t)^2 \sin(2\theta), \\ R(t) &= -\epsilon_0 s(t) \cos \theta \left(1 - \frac{3a_2}{a_3}\right) + \frac{4}{p}\epsilon_0^2 s(t)^2 \sin \theta \cot \lambda\end{aligned}$$

and ω_l^2 is defined in eq. (30).

5. – Lateral oscillations

As in the case of librations, we will obtain, from the original partial differential problem (see eqs. (17) or (23)), an ordinary differential problem in time only. In the following we do that separately for the two models of current presented in sect. 3.

5.1. Insulated tether. – In this case the relevant equations are eqs. (17). We now introduce the expansions

$$(32) \quad \xi_1(\tilde{z}, t) = \sum_{n=1}^{\infty} x_n(t) \phi_n(\tilde{z}), \quad \eta_1(\tilde{z}, t) = \sum_{n=1}^{\infty} y_n(t) \phi_n(\tilde{z})$$

in terms of the eigensolutions of the unperturbed system (*i.e.* the system with $I = 0$)

$$\phi_n(\tilde{z}) = \sqrt{2} \sin(k_n \tilde{z}), \quad k_n = n\pi, \quad n = 1, 2, \dots$$

Multiplying all terms in eqs. (17) by $\phi_n(\tilde{z})$, and integrating from $\tilde{z} = 0$ to $\tilde{z} = 1$, we obtain

$$(33) \quad \begin{aligned}\ddot{x}_n + k_n^2 p x_n &= -2\epsilon s(t) \sin \lambda \sin \theta \sum_{l=1}^{\infty} I_{nl} y_l, \\ \ddot{y}_n + (1 + k_n^2 p) y_n &= 2\epsilon s(t) \sin \lambda \sin \theta \sum_{l=1}^{\infty} I_{nl} x_l\end{aligned}$$

with

$$I_{nl} = \int_0^1 dz \phi_n(z) \frac{d\phi_l}{dz}.$$

It is easy to see that $I_{nl} \neq 0$ only when n and l have opposite parity. Therefore the n -th order in-plane modes are coupled to all the out-of-plane modes with parity different from n and vice versa. This excludes, in both equations, coupling terms almost resonating with the proper frequency of the corresponding oscillator.

5.2. *Bare tether.* – The relevant equations are eqs. (23). Expanding in series of the orthonormal modes, as in the previous section, we arrive at

$$(34) \quad \begin{aligned} \ddot{x}_n + k_n^2 p x_n &= -\epsilon_0 s(t) \sin \theta \sum_{l=1}^{\infty} \left(2h_{nl} + \frac{3}{2} g_{nl} \right) y_l, \\ \ddot{y}_n + (1 + k_n^2 p) y_n &= \epsilon_0 s(t) \sin \theta \sum_{l=1}^{\infty} \left(2h_{nl} x_l + \frac{3}{2} \tan \lambda \cos \theta g_{nl} y_l \right), \end{aligned}$$

where

$$g_{nl} = \int_0^1 dz \phi_n(z) \int_z^1 dz' \frac{\phi_l(z')}{(z')^{1/2}}, \quad h_{nl} = \int_0^1 dz (1 - z^{3/2}) \phi_n \frac{d\phi_l}{dz}.$$

Equations (34) are, again, an infinite system of coupled equations for all the different lateral modes. It is easy to realize, however, that, contrary to the case of the insulated tether, in-plane modes of any given order n are now coupled to out-of-plane modes of the same order. Due to the closeness of the proper frequencies of the two oscillators x_n and y_n (and due to the fact that the other frequencies contained in the terms on the right-hand sides of (34) are much smaller than the lateral frequencies), this implies that some of the coupling terms are almost resonating with the proper frequency of the corresponding oscillator. As we will see, this fact is of importance for stability.

6. – Instability mechanism

Before giving the results of a numerical analysis, let us note that eqs. (29) and (31), that we have derived for librations, if we neglect terms non-linear in the current, are both of the type

$$(35) \quad \ddot{x} + x = s(t) - f_x(t)y, \quad \ddot{y} + \hat{\omega}_2^2 y = r(t) + f_y(t)x,$$

where $\hat{\omega}_2 = \omega_2/\omega_1$, ω_1 and ω_2 being the unperturbed frequencies of the in-plane (x) and the out-of-plane (y) oscillator, respectively. The right-hand sides, which reflect the electrodynamic terms, contain both coupling terms (*i.e.* terms through which the in-plane motions are coupled to the out-of-plane motions and vice versa), and source terms, represented by $s(t)$ and $r(t)$. Let us first consider the effect of the coupling terms only. The functions $f_x(t)$ and $f_y(t)$ in (35) are both proportional to $\sin(\hat{\omega}_0 t)I(t)$ and, therefore, contain the beatings between the time variations due to the orbital motion and to the current. With the current variation envisaged (see eq. (12)), these beatings will produce frequencies 0, $\hat{\omega}_0$ and $2\hat{\omega}_0$ with the frequency 0 (*i.e.* a term constant in time) being produced only for $\phi \neq \pi/2$. In general, therefore, we can write

$$f_x(t) = -\beta [a_1 + b_1 \sin(\hat{\omega}_e t)], \quad f_y(t) = \beta [a_2 + b_2 \sin(\hat{\omega}_e t)]$$

with the frequency $\hat{\omega}_e$ being either $\hat{\omega}_0$ or $2\hat{\omega}_0$ and where the constant β can be written as

$$\beta = \frac{B_0 I_0}{m_t \hat{\omega}_1^2} \sin \lambda,$$

while the coefficients a_1 , a_2 , b_1 , b_2 will be different for the two cases of the bare and the insulated tether.

It can be seen that a system like (35), without source terms and with opposite signs in front of the electrodynamic forces in the two equations, which is the case in our problem, is unstable (see ref. [14] for detailed derivations). The instability is of a parametric type [15] and is made easier when one of the beat frequencies that we get on the right-hand side (through the products f_{xy} and f_{yx}) gets closer to the frequency of the unperturbed oscillator on the left-hand side of the corresponding equation. Explicit results are given in ref. [14].

Let us next consider the effect of the source terms only in eqs. (35). Clearly these terms alone cannot cause any instability. However, upon increasing the current, the response to these terms will of course be that of an increase in the oscillation amplitudes both in plane and out of plane.

In addition, these source terms, in the equations for the in-plane and out-of-plane oscillations, may contain frequencies which are close to the unperturbed frequencies of the corresponding oscillators. This is the case for a source term in the second of eqs. (29) and (31), referring to the out-of-plane librations, which exhibits a frequency $2\omega_0$ almost resonating with the frequency of the out-of-plane oscillator. This quasi-resonance induces a long-term modulation over the basic oscillations so that the structure of the out-of-plane solutions turns out to be that of a wave packet whose envelope has a period much longer than the orbital period.

Consider now the complete case which, for librations, includes in the electrodynamic forces both coupling and source terms. At small currents (or small values of β), the main effect on the solutions will be that of the source terms, because the coupling terms in eqs. (35) are proportional to x or y and, therefore, remain smaller than the source terms until x and y are small. Upon increasing the current, however, the source terms will induce larger oscillations (in particular this applies to the out-of-plane oscillations, with reference to the quasi-resonance mentioned above). At some point, *i.e.* above some value of the average current, the coupling terms in the two equations will become comparable with the source terms and then will become greater. From that point on, we should expect the instability phenomena due to coupling terms between in-plane and out-of-plane modes.

Therefore, for the case of librations, before going eventually to an unstable regime, we need to reach oscillations of a certain amplitude, so that the role of the coupling terms in the electrodynamic forces becomes significant.

The problem of lateral modes ((33) or (34)) is more complicated because each mode, of order n , is coupled to an infinity of other modes (in-plane and out-of-plane). However, the basic structure represented by (35) is still represented in the problem as we see, for example, by writing eqs. (34) only for mode $n = 1$. In addition, there are no source terms in the lateral problem. Hence, we expect again instability above a certain threshold in β . In addition, as the threshold gets smaller when one beat frequency on the right of each equation approaches the unperturbed frequency of the oscillator on the left side, we expect that bare tethers (where coupling between in-plane and out-of-plane modes of the same order and, therefore, almost of the same frequency, is possible) will show lower thresholds than insulated tethers for which, as we have remarked, in-plane modes of a given order are only coupled to out-of-plane modes of opposite parity and vice versa. In this case, the mismatch between beat frequencies on the right-hand sides of the equations and the unperturbed oscillator frequencies on the left sides will in fact be much higher.

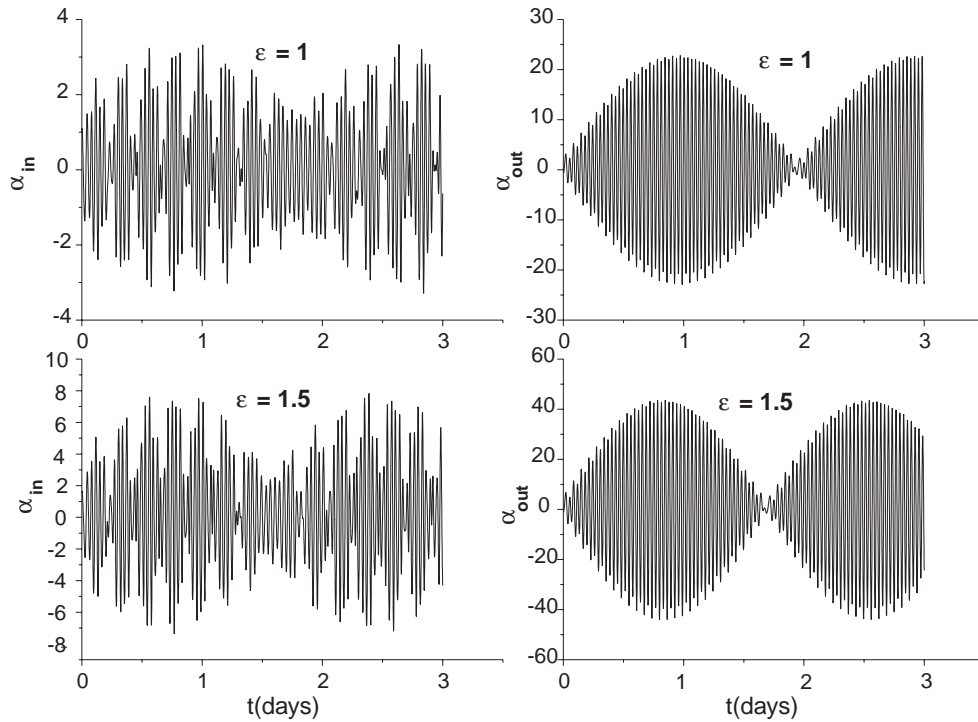


Fig. 1. – In-plane and out-of-plane libration angles for a bare tether as a function of time for two values of ϵ . The solutions refer to $\mu = 0.25$ and $\tilde{z} = 1$.

7. – Numerical results for libration modes

7.1. Bare tether. – As we have noticed earlier on, the tether dynamics depends only on two dimensionless parameters (ϵ and μ). Although we have obtained results for different values of μ , all the solutions that will be shown graphically in the paper refer to $\mu = 0.25$ (and several values of ϵ). This value, is obtained for a typical tether considered in previous deboost studies [2, 3], *i.e.* an Al tether of length $L = 5$ km and radius $r_w = 0.4$ mm, weighting ~ 7 kg and with a ballast mass $m_b \sim 30$ kg. In addition, in all the results reproduced (and also for lateral modes), we used $\delta = 0.5$ and $\phi = 0$ for the parameters characterizing the density modulation (and the corresponding modulation of the current).

For bare tether librations, fig. 1 gives a sequence of solutions of eqs. (31), corresponding to $\mu = 0.25$ and two values of ϵ . More specifically, what one finds plotted are the angles $\alpha_{in} \sim \xi_{0z}$ and $\alpha_{out} \sim \eta_{0z}$ (in degrees) as a function of time for a 3 day period. The angles refer to the termination $\tilde{z} = 1$ of the tether.

Notice, first of all, the wave packet behaviour of the out-of-plane oscillations. This is due, as was already anticipated, to a quasi-resonance between a frequency component $2\omega_0$ in the source term in the out-of-plane equation and the basic frequency of the out-of-plane oscillator. Indeed, for small values of ϵ , the period of the wave packet agrees with the one we can predict on the basis of the source term alone, while this period is seen in fig. 1 to decrease with increasing ϵ . We also point out that, if we look at the single coefficients for the cubic expansions for the displacements, we find that the coefficients

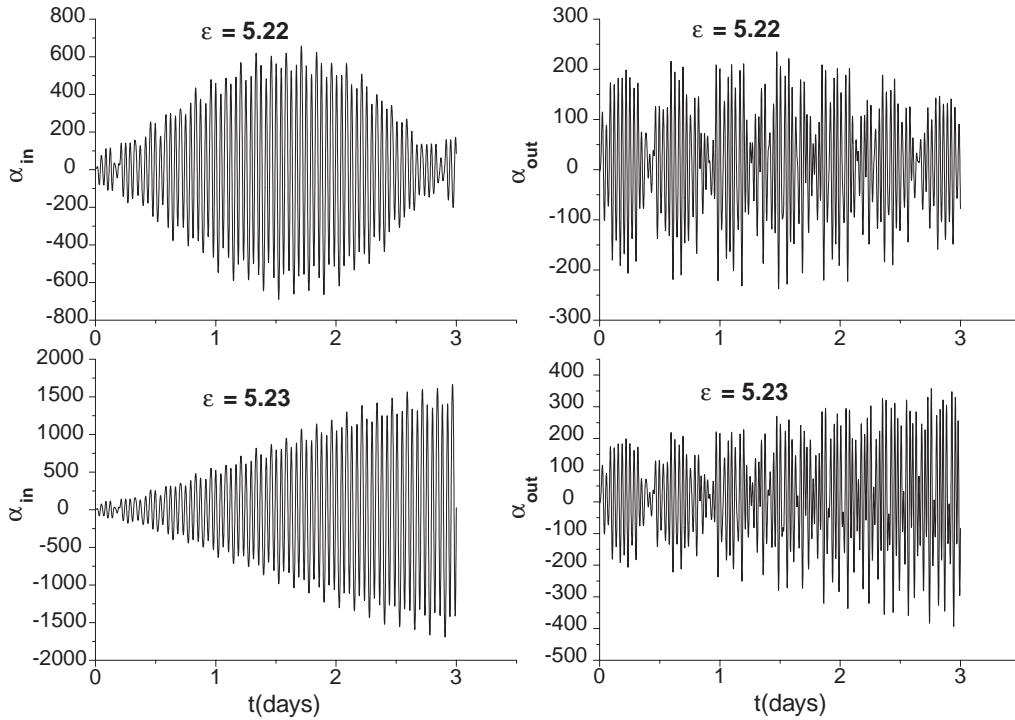


Fig. 2. – Transition to instability for the librations of a bare tether. The plots give libration angles as a function of time for two values of ϵ close to the transition and $\mu = 0.25$, $\tilde{z} = 1$.

x_3 and y_3 are much smaller than the others so that the shape of the tether during the oscillations is approximately parabolic.

Increasing ϵ , the maximum amplitude of the oscillations increases and, for $\epsilon = 1.5$, reaches $\sim 43.5^\circ$. Clearly, our linear approximation (implying $\xi_{0z} < 1$ and $\eta_{0z} < 1$) breaks down around these angles. Nonetheless, if we follow the behaviour of the system (31) for higher values of ϵ , we find a transition from oscillatory wave packet solutions to exponentially unstable solutions to occur between $\epsilon = 5.22$ and $\epsilon = 5.23$ as shown in fig. 2. For the tether parameters quoted above and an altitude of ~ 400 km, this corresponds to a threshold for the average current $I_0 \sim 1.6$ A. The transition occurs, however, well outside the validity of our linear approximation so that, on the basis of the present theory, we see that an instability can occur but we certainly cannot predict its threshold. Non-linearities should be necessarily taken into account.

A numerical analysis as a function of μ shows that the stability of the system increases upon decreasing μ , *i.e.* for given ϵ , lower values of μ give lower amplitude of the oscillations until the system becomes absolutely stable for $\mu = 0$.

As the solutions obtained vary on time scales much longer than the orbital period, it is appropriate to introduce in the calculations also the effect of the magnetic tilt, *i.e.* the variation of λ with time given in eq. (13). We have done that and found, however, that the inclusion of the slow modulation of λ introduces only slight differences to the results obtained previously.

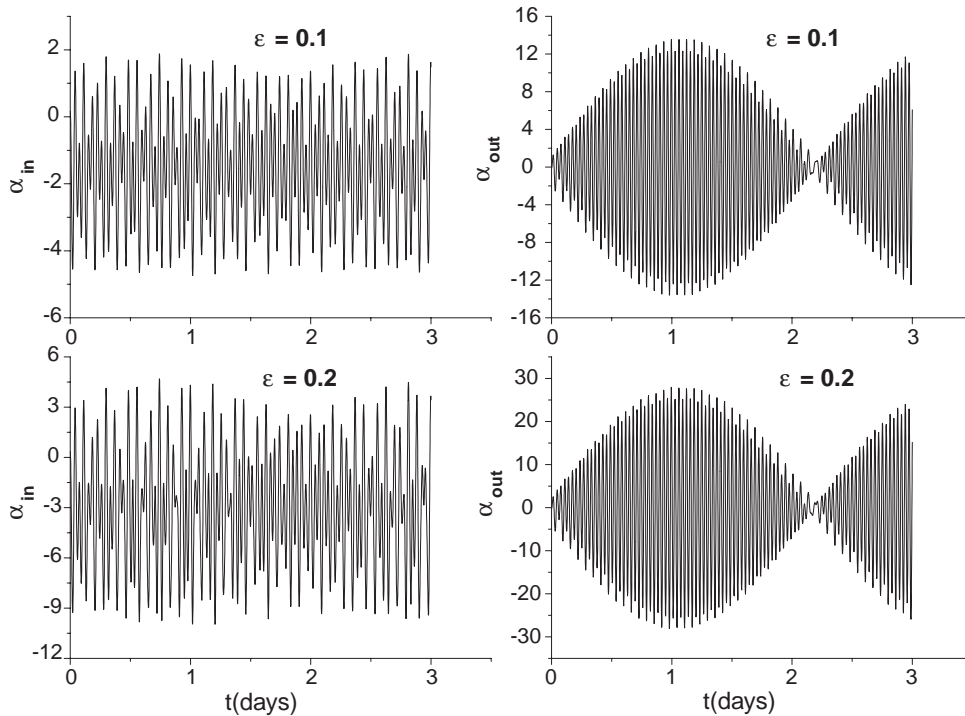


Fig. 3. – In-plane and out-of-plane libration angles for an insulated conducting tether and two values of ϵ . The solutions refer to $\mu = 0.25$ and $\tilde{z} = 1$.

7.2. Insulated tether. – If we compare eqs. (29), for the librations of the insulated tether, with eqs. (31) referring to a bare tether, we see that the main difference stands in the coefficients multiplying the electrodynamic terms linear in ϵ , which are larger in the first than in the second case. Because of this, we expect that, for the insulated tether, a given maximum amplitude in the oscillations will be reached at lower values of ϵ (with respect to the case of the bare tether).

This is confirmed by numerical solutions of eqs. (29). Figure 3 is a sequence of such solutions, for the in-plane and out-of-plane angles, corresponding to $\mu = 0.25$ and $\tilde{z} = 1$, and should be compared with the sequence of fig. 1 corresponding to the bare tether. We see that, at $\epsilon = 0.2$, we have reached amplitudes of the α_{out} solution already higher than those obtained for $\epsilon = 1$ in the case of the bare tether. At $\epsilon = 0.2$, we reach in fact $\alpha_{outmax} \sim 27^\circ$ and, for higher values of ϵ , we start going out of the validity of our theory.

The transition from an oscillatory to an unstable behaviour (which we do not show) is found to occur between $\epsilon = 2.6$ and $\epsilon = 2.8$ (the corresponding value for the case of the bare tether was $\epsilon \sim 5.22$) with the oscillations being amply above the limits of the linear approximation.

Although, as in the case of the bare tether, we cannot put any confidence in this threshold, we seem nonetheless to have the indication that an insulated tether is more easily unstable, with respect to librations, than a bare tether.

There is, finally, a further case which is worth to be studied and is that of a current which is also constant in time, as it can be obtained with an electronic limitation. Notice

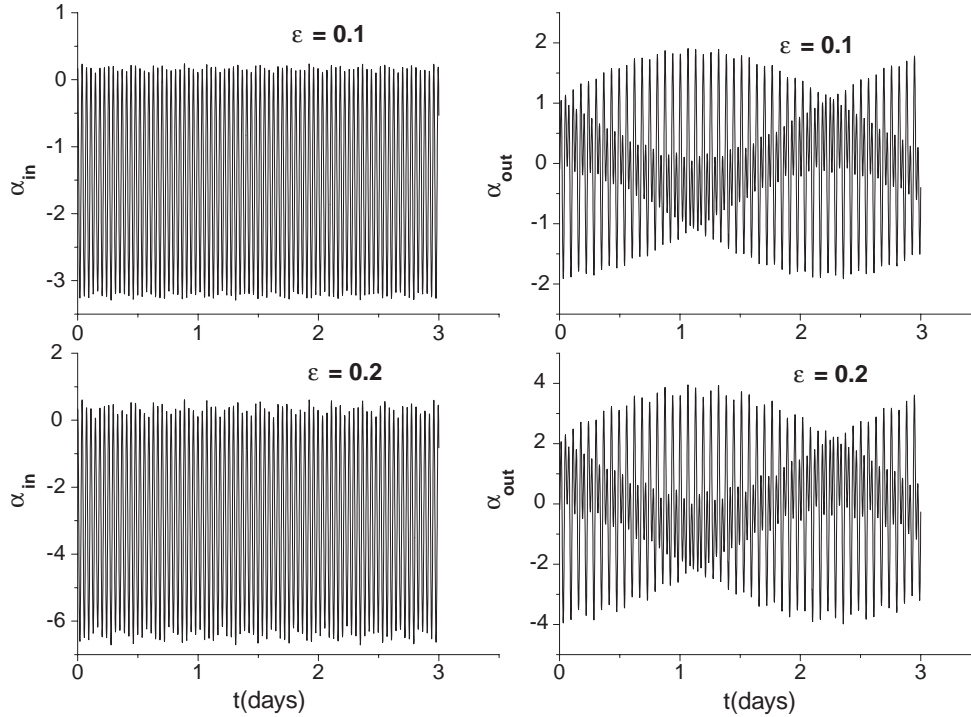


Fig. 4. – In-plane and out-of-plane libration angles for an insulated conducting tether with the current kept electronically constant in time. The plots refer to two values of ϵ , $\mu = 0.25$ and $\tilde{z} = 1$.

that this case is appropriate only for the insulated conducting tether (hence eqs. (29)), whereas, for a bare tether, with a current limitation, we would in general find the current to be equal to the limiting value only at the satellite end, while, along the tether, the current would vary both in time and along the tether length (staying always smaller than the imposed value).

For the case of a current constant in time, the electrodynamic terms in eqs. (29) vary in time only because of the orbital variations. The beatings between variations of the current and orbital variations are absent. As these beatings can provide frequencies close to the basic frequencies of the in-plane and out-of-plane oscillators, and these favors the oscillation growth, we expect that the oscillations amplitude will grow with ϵ (for given μ) at a much lower rate. In particular, the quasi-resonance in the out-of-plane motions that we have encountered previously, would now be absent and, therefore, α_{out} will oscillate in a manner similar to α_{in} without any wave packet behaviour.

Figure 4 shows the angles α_{in} and α_{out} which are obtained for $\epsilon = 0.1$ and $\epsilon = 0.2$ for a current constant in time and should be compared with fig. 3 (both cases refer again to $\mu = 0.25$ and $\tilde{z} = 1$). We see that, with respect to the case of an oscillating current, we obtain now a lower amplitude of the oscillations (in particular those out of plane). Thus, making $I = \text{const}$, renders the insulated tether more stable. A transition to instability is found to occur at $\epsilon \sim 5$ but, again, outside the validity of the linear approximation.

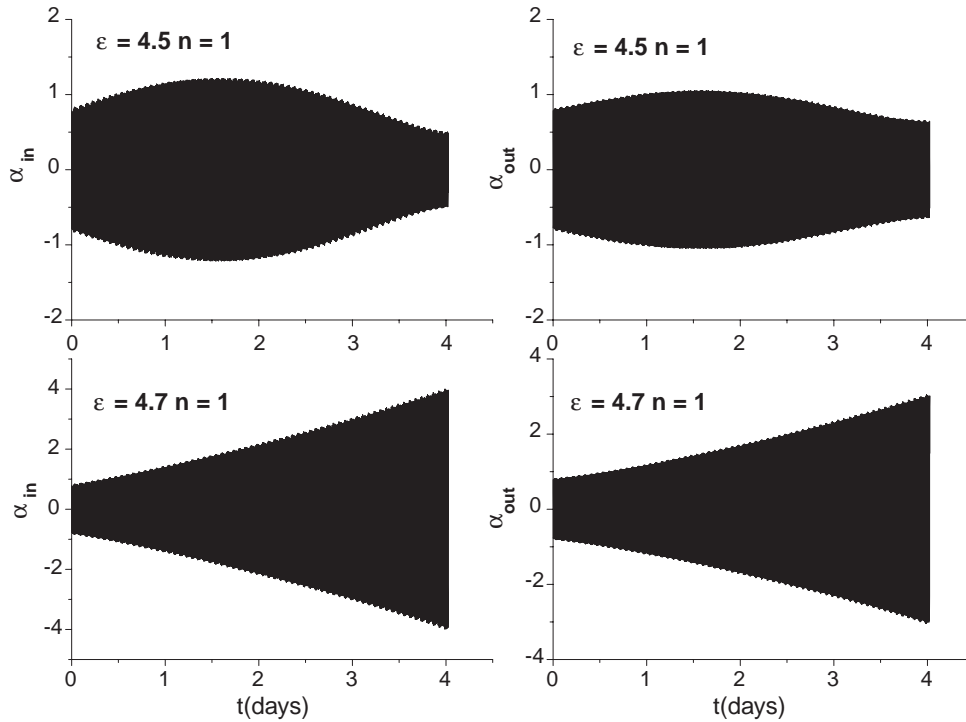


Fig. 5. – Transition to instability of the $n = 1$ lateral mode of a bare tether, with coupling to mode $n = 2$ taken into account. The solutions refer to two values of ϵ , $\mu = 0.25$ and $\tilde{z} = 0.4$.

8. – Numerical results for lateral modes

8.1. Bare tether. – For the case of bare tethers (see eqs. (34)), in-plane modes of order n are coupled to out-of-plane modes of the same order and vice versa so that there are coupling terms on the right-hand sides of the dynamical equations which oscillate at about the same frequency as the unperturbed oscillators on the left-hand sides.

Figure 5 gives the results obtained from numerical solutions of eqs. (34), including modes $n = 1$ and $n = 2$. More precisely the 4 panels give the time variation of the in-plane and out-of-plane oscillations (in degrees), due to the $n = 1$ mode for two values of ϵ . The angles are calculated at $\tilde{z} = 0.4$. It is clear that, in going from the value $\epsilon = 4.5$ (upper two panels) to $\epsilon = 4.7$ (lower two panels), the nature of the solutions changes (for both α_{in} and α_{out}) from oscillatory to growing. We need in fact a rather long integration time (4 days in the figure), to appreciate the transition. In a smaller period (for example a 1 day integration), we would judge the oscillations growing also for $\epsilon = 4.5$. Indeed, due to the rather long integration time (in comparison with the period of the $n = 1$ mode), what we see is just the envelope of the oscillations which would be resolved only by plotting much shorter periods.

As for mode $n = 2$, which is also included in the same calculation, the next figure 6 shows what we obtain for the angular oscillations coming from $n = 2$, in the same time interval and for $\epsilon = 4.7$. Contrary to mode $n = 1$ (see the lower two panels of fig. 5), the mode $n = 2$ seems to have a periodic behaviour in the time frame considered. However,

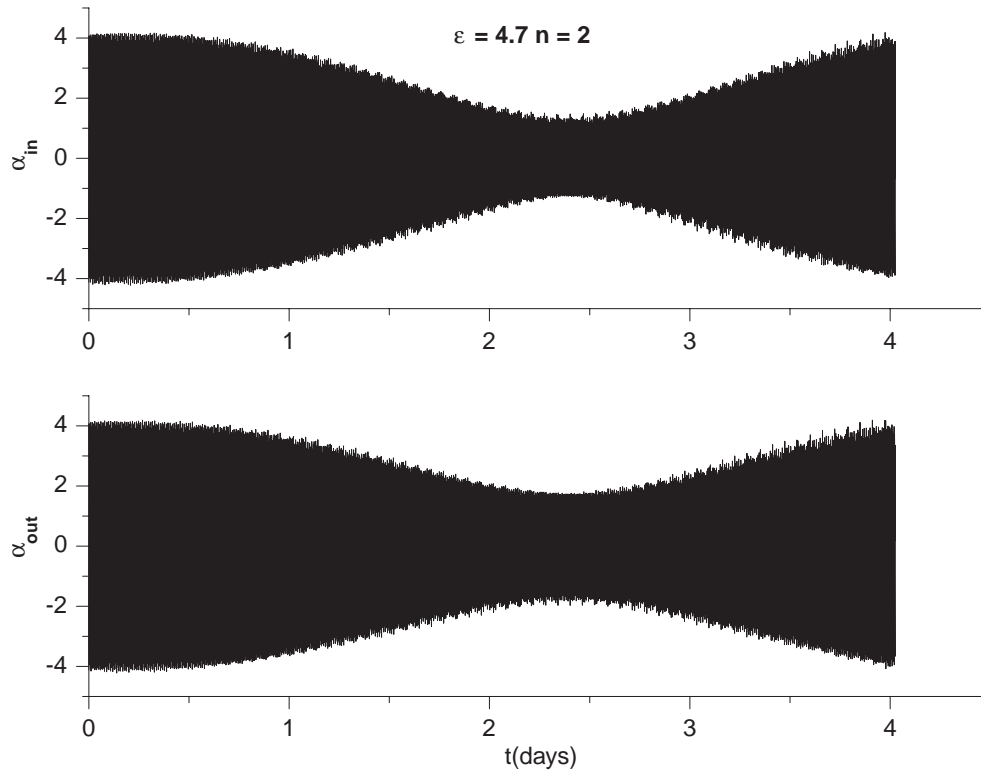


Fig. 6. – In-plane and out-of-plane angles *vs.* time for the lateral mode $n = 2$ of a bare tether with mode $n = 1$ also included. The solutions refer to $\epsilon = 4.7$, $\mu = 0.25$ and $\tilde{z} = 0.4$.

on longer times, we would find that also mode $n = 2$ is growing due to the coupling with mode $n = 1$ in the equations.

In conclusion, for a bare tether and in linear theory, we find an instability of lateral modes occurring at $\epsilon \sim 4.6$ (for $\mu = 0.25$), which would correspond, at 400 km, to an average current $I_0 \sim 1.5$ A. Notice that, as we see from the lower two panels of fig. 5, the instability starts at low values of the angles which are now (contrary to the libration case), consistent with our linear approximation.

Finally, the inclusion of mode $n = 3$ in the calculation, of which we do not report the results, does not change appreciably the results that we have shown.

8.2. Insulated tether. – As already noticed in subsect. 5.1, eqs. (33) for the insulated tether are such that, for example, the in-plane modes of order n are coupled, via the electrodynamic forces, to all the out-of-plane modes of parity different from n and, likewise, for the out-of-plane modes. This implies that the frequencies appearing in the coupling terms on the right-hand sides of eqs. (33) are radically different from the frequency of the n -th oscillator, appearing on the left-hand sides and no parametric resonance can occur.

Therefore, on the basis also of the comments given in sect. 6, we do not expect the lateral modes, for the insulated conducting tether, to be easily unstable (*i.e.* unstable for moderate currents). This is confirmed by numerical solutions of eqs. (33), reported in

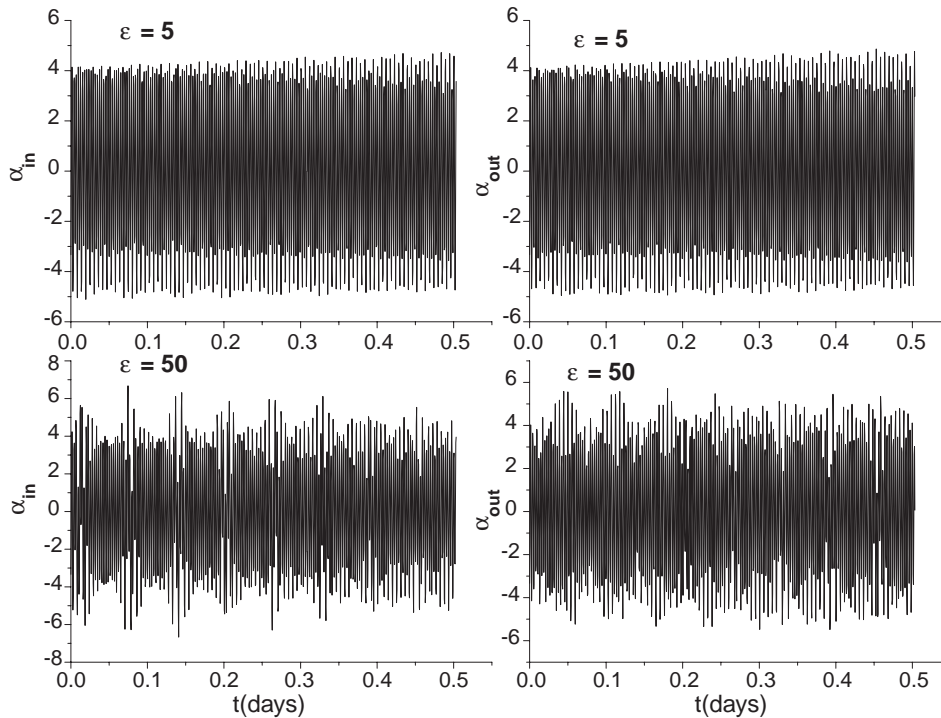


Fig. 7. – In-plane and out-of-plane angles *vs.* time for the lateral modes of an insulated conducting tether for two values of ϵ , $\mu = 0.25$ and $\tilde{z} = 0.4$ (modes 1 and 2 included).

fig. 7, and corresponding to the case where we have truncated the infinite system (33) to $n = 2$ (*i.e.* we have included the modes $n = 1$ and $n = 2$). The first two panels of fig. 7 correspond to $\epsilon = 5$ (a value which is above the instability threshold for the bare tether lateral modes). The angles, both in plane and out of plane (in degrees and calculated at $\tilde{z} = 0.4$), stay quite small in the integration period which is shown (0.5 days) and continue to do so on longer times. The lower two panels in fig. 7 refer to $\epsilon = 50$ and, as we see, the oscillation amplitude has only slightly increased with respect to the previous case. Therefore, as expected, the insulated tether, at least in linear theory, is quite stable with respect to lateral oscillations. We find that instability is eventually reached only for $\epsilon \sim 65$ (for $\mu = 0.25$).

Finally, it has also been checked that no significant modifications are obtained by truncating the system (33) at orders higher than $n = 2$.

9. – Discussion

Let us summarize what we have done and what we have found. We have investigated the dynamics of a flexible conducting tether, in the presence of electrodynamic forces, in the linear approximation. For this reason, longitudinal oscillations, which are second order, were not considered. Furthermore, because of their different frequencies, we were able to separate the problem of tether librations from that of the lateral modes.

For the libration modes, and both for the case of the insulated conducting tether

and the case of the bare tether, we have found instability above a certain threshold in the parameter ϵ . What happens, starting from small current values, is that, initially, the electrodynamic source terms in the equations dominate over the coupling terms and lead, upon increasing the current, to an increase in the amplitude of the oscillations (starting with the oscillations out of plane). At some point, the coupling terms become dominant. It is these coupling terms, which may contain frequencies close to the natural frequencies of the in-plane and out of plane unperturbed oscillators, which lead to instability.

In both the cases of the bare and the insulated tether, the transition to instability occurs for amplitudes of the oscillations ($\sim 40^\circ$) which are outside the validity of the linear approximation. As a consequence, we cannot put any confidence in the threshold values obtained for ϵ (or the average current I_0). We do have however the indication that, in linear theory, insulated tethers are more easily unstable than bare tethers in that oscillations of comparable amplitudes are reached at smaller current values.

Instability above a certain threshold in ϵ is also found for the lateral modes. There, however, also at instability onset, the amplitude of the in-plane and out-of-plane oscillations is small and therefore consistent with the linear approximation. Insulated tethers, where coupling occurs in the equations only between modes of opposite parity, are found to be much more stable, with respect to lateral modes, than bare tethers, at least in the framework of the linear approximation.

In conclusion, it is clear that, in particular for the case of librations, before drawing any conclusion, we should go to a non-linear treatment. This necessity is also indicated by the work of Pelaez *et al.* [8], concerning librations of a rigid tether, where they demonstrate that the inclusion of non-linearities produces an inherent instability, *i.e.* the tether oscillations necessarily grow however small is the current.

If, in spite of the limitations of linear theory, we refer to the average current thresholds found for bare tethers and lateral modes, which are of the order of 1.4 A (for $\mu = 0.25$), we see that average currents of this order are obtained in the range of altitudes from ~ 600 km downwards. Hence, it appears that, if we want to use electrodynamic tethers to deorbit spacecraft, some current control will have to be exercised at these low altitudes. This will lengthen the deorbiting time (with respect to the values obtained in [2,3]), but not much because the longest part of deorbiting is that above those altitudes where the ionospheric density, and, hence, the current, is smaller.

On the other hand, for the application of electrodynamic tethers to upboost spacecraft, and, in particular, the International Space Station (ISS), we in general need to have currents much above 1 A (for example of the order of 10 A) to compensate for the decay due to the atmospheric drag. This means that a light tether system, as the typical one we have referred to in this paper, will not be suitable but we will need, on the one hand, to increase the tether cross-section (for equal length), to obtain higher currents and, on the other hand, to increase the ballast mass m_b to remain stable. Adding mass, which would certainly be a problem for the application of deboost, might, on the other hand, not be a problem for upboost, in particular with reference to ISS.

REFERENCES

- [1] ANSELMO L., ROSSI A. and PARDINI C., *Adv. Space Res.*, **23** (1999) 201.
- [2] DOBROWOLNY M., VANNARONI G. and DE VENUTO F., *Nuovo Cimento C*, **23** (2000) 85.
- [3] VANNARONI G., DOBROWOLNY M. and DE VENUTO F., *Space Debris*, **1** (2001) 159.

- [4] BALLANCE J. and JOHNSON L., *Propulsive Small Expendable Deployer System (ProSEDS)*, in *Proceedings of Space Technology and Applications International Forum (STAIF 2001)*, edited by M. EL GENK, *AIP Conference Proceedings*, Vol. **552** (American Institute of Physics, New York) 2001, pp. 419-424.
- [5] DOBROWOLNY M. and STONE N., *Nuovo Cimento C* **17** (1994) 1.
- [6] ANGRILLI F., BIANCHINI G., DA FORNO R. and FONTI G., *Active and passive damping of tethered systems*, in *Proceedings of the Fourth International Conference on Tethers in Space, April 1995* (Smithsonian Institution, Washington D.C.), Vol. **1**, p. 419.
- [7] LORENZINI E. C., ESTES R. D., COSMO M. L. and PELAEZ J., *Dynamical, electrical and thermal coupling in a new class of electrodynamic tethered systems*, in *Spaceflight Mechanics 2000*, Vol. **102**, *Advances in the Astronautical Sciences*, edited by R. H. BISHOP, D. L. MACKISON, R. D. CULP and M. J. EVANS 1999, paper AAS99-192.
- [8] PELAEZ J., LORENZINI E. C., LOPEZ-REBOLLAL O. and RUIZ M., *A new kind of dynamic instability in electrodynamic tethers*, in *AAS/AIAA Space Flight Mechanics Meeting, ClearWater, Florida, January 2000*, Paper AAS 00-190.
- [9] PELAEZ J., RUIZ M., LOPEZ-REBOLLAL O., LORENZINI E. C. and COSMO M. L., *A two bar model for the dynamics and stability of electrodynamic tethers*, in *AAS/AIAA Space Flight Mechanics Meeting, ClearWater, Florida, January 2000*, Paper AAS 00-188.
- [10] MISRA A. K. and MODI V. J., *A survey on the dynamics and control of tethered satellite systems*, in *Tethers in Space*, edited by P. M. BAINUM, I. BEKEY, L. GUERRIERO and P. A. PENZO, Vol. **62**, *Advances in Astronautical Sciences*, Paper AAS-86-246, 1986.
- [11] HE X. and POWELL J. D., *Tether damping in space*, in *Space Tethers for Science in the Space Station Era, Venice, October 1987*, edited by L. GUERRIERO and I. BEKEY, *Proc. SIF*, vol. **14** (Editrice Compositori, Bologna) 1988, p. 153.
- [12] CAMPBELL W. H., *Introduction to Geomagnetic Fields* (Cambridge University Press) 1997.
- [13] SCHOTT L., *Electrical probes*, in *Plasma Diagnostics*, edited by W. LOCHTE-HOLTGREVEN (North Holland Publishing Company, Amsterdam) 1968.
- [14] DOBROWOLNY M., *Electrodynamic tether stability: linear theory*, Internal Report IFSI-2001-4, March 2001.
- [15] NAYFEH A., *Perturbation Methods* (John Wiley and Sons) 1973.